International Journal of Nanomedicine

Dovepress
open access to scientific and medical research

Open Access Full Text Article

ORIGINAL RESEARCH

Effects of light irradiation upon photodynamic therapy based on 5-aminolevulinic acid–gold nanoparticle conjugates in K562 cells via singlet oxygen generation

Hao Xu
Chen Liu
Jiansheng Mei
Cuiping Yao
Sijia Wang
Jing Wang
Zheng Li
Zhenxi Zhang

Key Laboratory of Biomedical Information Engineering of Education Ministry, Institute of Biomedical Analytical Technology and Instrumentation, School of Life Science and Technology, Xi'an Jiaotong University, Xi'an, Shannxi, People's Republic of China

Purpose: As a precursor of the potent photosensitizer protoporphyrin IX (PpIX), 5-aminolevulinic acid (5-ALA), was conjugated onto cationic gold nanoparticles (GNPs) to improve the efficacy of photodynamic therapy (PDT).

Methods: Cationic GNPs reduced by branched polyethyleneimine and 5-ALA were conjugated onto the cationic GNPs by creating an electrostatic interaction at physiological pH. The efficacy of ALA-GNP conjugates in PDT was investigated under irradiation with a mercury lamp (central wavelength of 395 nm) and three types of light-emitting diode arrays (central wavelengths of 399, 502, and 621 nm, respectively). The impacts of GNPs on PDT were then analyzed by measuring the intracellular PpIX levels in K562 cells and the singlet oxygen yield of PpIX under irradiation.

Results: The 2 mM ALA-GNP conjugates showed greater cytotoxicity against K562 cells than ALA alone. Light-emitting diode (505 nm) irradiation of the conjugates caused a level of K562 cell destruction similar to that with irradiation by a mercury lamp, although it had no adverse effects on drug-free control cells. These results may be attributed to the singlet oxygen yield of PpIX, which can be enhanced by GNPs.

Conclusion: Under irradiation with a suitable light source, ALA-GNP conjugates can effectively destroy K562 cells. The technique offers a new strategy of PDT.

Keywords: nonradiative energy transfer, photodamage, protoporphyrin IX, selective destruction, singlet oxygen sensor green reagent, surface plasmon resonance

Introduction

Photodynamic therapy (PDT) is a minimally invasive therapeutic modality approved for cancer treatment and some other nononcological disorders.[1] In PDT, a photosensitizer (PS) with photosensitizing properties is selectively accumulated in malignant tissue. When the malignant tissue is exposed to light with a specific wavelength, the PS is activated from its ground singlet state to an excited singlet state, after which it undergoes intersystem crossing to an excited triplet state. Some PS molecules, when they are in the excited state, release energy through physical processes. This energy produces fluorescence and phosphorescence that can be used for diagnosing disease. Other PS molecules are transferred to biological substrates and molecular oxygen to generate reactive oxygen species (ROS) and singlet oxygen, which are responsible for tumor regression and the cytotoxicity of neoplastic cells.

Correspondence: Zhenxi Zhang
Director, Institute of Biomedical Analytical Technology and Instrumentation, School of Life Science and Technology, Xi'an Jiaotong University, 28 Xianning Xi Road, Xi'an 710049, People's Republic of China
Tel +86 29 8266 6854
Fax +86 29 8266 6854
Email zxzhang@mail.xjtu.edu.cn

Improving the efficacy of PDT requires three elements: a PS, a light source, and tissue oxygenation.[2] Although the concentration of oxygen in tissue depends solely on tissue status,[3] studies should explore novel photosensitizers and more suitable light resources to improve the effect of photodynamic therapy.

The first generation PSs used in PDT were hematoporphyrin and derivative hematoporphyrin. Although some of these compounds have been approved in application, they are far from an ideal PS due to their significant limiting factors for chemotherapeutics and radiotherapy.[1] For these reasons, research on PDT has been focused on the development of alternative new-generation PSs with improved physical, chemical, and therapeutic properties.

The pro-photosensitizing metabolite 5-aminolevulinic acid (ALA) has attracted significant attention.[4] ALA is a natural precursor of protoporphyrin IX (PpIX) in the heme biosynthetic pathway. Under normal physiological conditions, heme synthesis from glycine through PpIX is regulated by negative feedback control of the enzyme ALA synthase by free heme; thus, the concentration of ALA or PpIX in normal tissue is sufficiently low to preclude cell damage that can occur by photochemical reactions. In contrast, in tumor tissues, the regulatory feedback system is bypassed as the administration of exogenous ALA causes excess cellular accumulation of downstream metabolites.[5] Due to the importance of heme synthesis in ALA-PDT, we chose the K562 human erythroleukemic cell, which is a well-known model for heme synthesis because erythroid cells produce 95% of total heme,[6] in order to significantly enhance the efficacy of ALA-PDT. The detailed mechanism of ALA-PDT cytotoxic effects on K562 cell line has been described previously.[7]

The hydrophilic nature of ALA may limit its ability to penetrate skin or cell membranes and thereby restrict the effectiveness of ALA-PDT.[8] Gold nanoparticles (GNPs) have high available surface activity[9] and good biocompatibility,[10,11] which allows exploitation of their unique chemical and physical properties for transporting and unloading pharmaceuticals.[12] The use of GNPs as carriers for PS delivery represents a promising approach to enhance the efficacy of PDT.[13–17]

As nanosized particles, GNPs can be delivered to and accumulate in tissues with permeable vasculature due to the enhanced permeability and retention (EPR) effect.[18] Given that tumor tissues are known to exhibit highly enhanced vascular permeability,[19] GNPs can passively accumulate in tumor tissues through the rich permeable vasculature.[20]

In addition to the EPR effect, some studies have indicated that cationic GNPs show facilitated binding to negative tumor cell membranes.[14] Moreover, GNPs can adsorb onto leukemia K562 cells through the weak interaction between the nanoparticles and mercapto or primary amine groups on the cell membrane.[21] Accordingly, we chose cationic GNPs as carriers to deliver drugs to bind to leukemia K562 cells, which have a negative surface charge.[22]

In addition, in recent demonstrations combining nanomaterials with PSs, GNPs not only facilitated delivery of PS to tumor cells but were also better for enhancing the singlet oxygen yield of PpIX.[13,14] The ability of PpIX to generate singlet oxygen is one of the most important factors for evaluating the PDT effect.[23] Thus, a compatible light source can be used to excite the optical properties of GNPs to improve the singlet oxygen yield of a PS.

In this study, we synthesized cationic GNPs by in situ chemical reduction of $HAuCl_4$ with the use of branched polyethyleneimine (BPEI) as a reductant and stabilizer.[24] We then conjugated 5-ALA onto the cationic GNPs through an electrostatic interaction under physiological pH (pH 7.2–7.6). We also investigated the efficacy of ALA-GNP conjugates under irradiation by LEDs and a mercury lamp, and measured the singlet oxygen yield of PpIX to analyze the influence of GNPs on the PS.

Materials and methods

Materials

ALA, PpIX, and BPEI were purchased from Sigma-Aldrich (St Louis, MO), 4-(2-hydroxyethyl)-1-piperazineethane-sulfonic acid (HEPES) and $HAuCl_4$ were purchased from Dingguo Co (Beijing, China), 1% penicillin/streptomycin, phosphate-buffered saline (PBS) and sodium dodecyl sulfate (SDS) lysis buffer were purchased from Beyond Ltd (Haimen, China), fetal bovine serum (FBS) and RPMI1640 were purchased from Thermo Fisher Scientific (Waltham, MA), Cell Counting Kit-8 (CCK-8) was purchased from Dojindo (Kumamoto, Japan) and Singlet Oxygen Sensor Green reagent (SOSGR) was purchased from Invitrogen (Carlsbad, CA).

Synthesis and characterization of ALA-GNP conjugates

Different molar ratios of 0.1% $HAuCl_4$ and BPEI (molecular weight = 25,000) were mixed and stirred in ultrapure water at 80°C to prepare a series of GNPs, and solutions were collected until the color changed from yellow to dark red upon completion of the reduction reaction. The GNPs were

then washed with ultrapure water and purified twice by centrifugation at 25,000 × *g* for 30 min at 4°C. 5-ALA was dissolved in 20 mM HEPES to adjust the pH value to 7.2–7.4, after which it was filtered with a 0.2-μm filter. The colloidal GNPs were also filtered with a 0.2-μm filter. Subsequently, the ALA solution and GNP colloidal solution were mixed at a number of ratios to prepare the conjugates.

Ultraviolet-visible (UV-Vis) absorption spectra were measured using a DU-640 UV-Vis spectrophotometer (JASCO, Tokyo, Japan). Transmission electron microscopy (TEM) images were acquired on a JEM-200CX transmission electron microscope (Hitachi, Tokyo, Japan). The average diameter of the GNPs and conjugates were examined using a ZetaSizer Nano ZS90 (Malvern Instruments, Malvern, UK). This device was also used to measure the zeta-potential after GNP and conjugate solutions were further adjusted to pH 7.4 with 1 N NaOH.

Light source

Light-emitting diodes (LEDs) have been used for PDT due to their great advantages of convenience, stability, and broad-spectrum properties.[25] We thereby used LEDs in this study. A mercury lamp irradiation system, which caused significant photodamage to tumor cells in research on ALA-PDT,[26] was also adopted to compare the PDT results with those after LED irradiation. Preliminary studies have indicated that a low light dose irradiation can induce cell death via a slower mechanism with its gentler thermal effect. Chen et al reported that a light dose of 1.44 J/cm^2 on cells incubated with gold nanoshells was optimal for reducing cell viability.[27] Here, we used an LED source (Hangke Co, Hangzhou, China) and a 400-W mercury arc lamp (Yaming Co, Shanghai, China) with the same light dose of 3.6 J/cm^2, but different values of full width at half-maximum to comprehensively explore the efficacy of ALA-GNP conjugates in PDT.

Mercury lamp irradiation was generated with a Spiegel condenser illuminated by a mercury lamp (Yaming Co, Shanghai, China), filtered with interference filters (Haiguang Co, Shanghai, China) of 410 nm (bandwidth = 10 nm), and attenuated by a lens. An energy fluence rate of 1 mW/cm^2 was obtained by adjusting the distance between the lens and sample cells. Previous work on ALA in our lab has demonstrated that irradiation with 410 nm caused maximum photodamage to the membrane and mitochondrial function of HL60 cells.[26]

We adopted three types of LEDs. Purple LEDs (central wavelength = 398 nm) were chosen to contrast with the mercury lamp. Green LEDs (central wavelength = 505 nm), which fit the absorption wavelength of GNPs, can excite photic properties such as surface plasmon resonance. Red LEDs (central wavelength = 621 nm), which have better penetration depth, display significant efficacy in PDT.[28] The LED light sources were created with a diode array system containing 96 LED units with maximum emission. The energy fluence rates of these light sources were adjusted to 1 mW/cm^2 using a variable resistor in series.

The energy fluence rates of these light sources were measured using a 3-sigma laser power meter (Coherent Inc, Portland, OR). The emission spectra of the light sources (Figure 1) were detected using a HR4000 high-resolution spectrometer (Ocean Optics Inc, Dunedin, FL).

Cell culture

We used the chronic myelogenous leukemia cell line K562 (provided by Northwest University, Xi'an, China). RPMI1640 supplemented with 10% FBS and 1% penicillin–streptomycin was used as the cell-culture medium. The cells were cultured at a humidified atmosphere of 37°C with 5% CO_2 in a HERAcell 150 Copper CO_2 incubator (Thermo Fisher Scientific) and subcultured every 3 days.

Photodynamic therapy in vitro

To five 96-well plates, we added the same cells and drugs as follows: 100 μL serum-free cell suspensions per well (cell density of 10^6/mL) were seeded in several 96-well plates. ALA, ALA-GNP conjugates, and GNPs were freshly prepared at three concentrations (3, 2, and 1 mM each) and respectively added to the cell suspensions in different wells for the drug groups. A drug-free cell suspension was used for the control group. Every group had three duplicate samples.

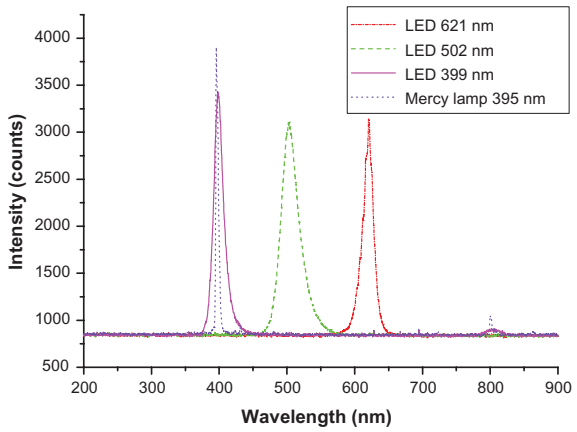

Figure 1 The emission spectra of all the light sources.
Note: Peak is the central wavelength of light sources.

All 96-well plates containing cells were incubated with the medium containing different reagents for 4 hours under dark conditions. Four plates were irradiated by the mercury lamp and three types of LEDs for 1 hour each. At the same time, another 96-well plate containing cells was used as the control under dark treatment.

Cell viability

After irradiation treatment, the cell suspensions in all 96-well plates were centrifuged at 400 × *g* for 5 minutes and washed twice with PBS to remove free drug. The cells were then refreshed with 100 μL of cell-culture medium containing 10 μL of the CCK-8. After incubation for 24 hours, cell numbers were measured as the absorbance (450 nm) of reduced WST-8 (2-(2-methoxy-4-nitrophenyl)-3-(4-nitrophenyl)-5-(2,4-disulfophenyl)-2H-tetrazolium, monosodium salt) by using a MK3 96-well microplate reader (Labsystems, Vantaa, Finland).

Measurement of PpIX formation and singlet oxygen generation

For PpIX detection, K562 cell suspensions (cell density of 10^6/mL) were seeded in 6-well plates. The medium of the cell-seeded well plates was then replaced with a serum-free medium containing 2 mM ALA, GNPs, or ALA-GNP conjugates. Untreated cells were used as the drug-free control. Cells were treated with the drug-containing medium under dark conditions. Homogeneous aliquots of cells were withdrawn from 6-well plates at 0, 3, 4, 6, and 8 hours, respectively. Cell suspensions were washed twice with PBS to remove free drug lysed in SDS lysis buffer, and then shaken for 10 minutes. Cell lysates were centrifuged at 12,000 × *g* for 5 minutes, and the fluorescence intensity was measured using an F-4500 fluorescence spectrophotometer (Hitachi). The excitation waveband was 410 nm, and the emission spectra were scanned from 420 to 700 nm. The peak fluorescence value at 631 nm was used for kinetic measurements.

SOSGR was used as the singlet oxygen-tracking agent. Given that SOSGR is cell-impermeable, 100 μL of GNP solution was directly mixed with 50 μL of 200 μM PpIX in cell-free solution to study the effect of GNPs on singlet oxygen generation of PpIX. Next, 20 μL of 100 μM SOSGR and ultrapure water were added to obtain the final 1000-μL sample solution. The PpIX alone, GNP alone, and drug-free groups were also prepared in the same manner. Irradiation treatment was performed by exposing the sample to red LEDs and green LEDs for different durations. The fluorescence measurement of SOSGR was performed using an F-4500 fluorescence spectrophotometer (Hitachi) at an excitation wavelength of 488 nm.

Statistical analysis

The experiments were performed at least three times. Data are shown as the mean ± standard error of independent experiments. The means were compared using Student's *t*-test, and differences were considered statistically significant at $P < 0.001$.

Results

Characterization of cationic GNPs

BPEI is a type of polyelectrolyte that serves as a reductant, stabilizer, and linker for preparing GNPs.[24] The secondary amine of BPEI has a strong reducing ability, readily forming ion pairs with $AuCl_4^-$ anions to produce zero-valent gold atoms.[29] The gold atoms can then collide with each other to form GNPs. In contrast, the amine groups of BPEI, which associate with the particle surface, prevent further growth of GNPs. Therefore, when BPEI and $HAuCl_4$ are mixed at a suitable ratio, GNPs with low-dispersing and uniform distribution can be prepared. In addition, due to the positive charge of the amine group on BPEI, this type of GNP is positively charged.

The absorption spectra of GNPs showed little difference when mole ratio of $HAuCl_4$ and BPEI were changed (Figure 2). With increased BPEI, absorbance peaks showed a small red shift around 530 nm. This absorbance peak was caused by transverse surface plasma absorption of GNPs. Moreover, longitudinal surface plasma absorption

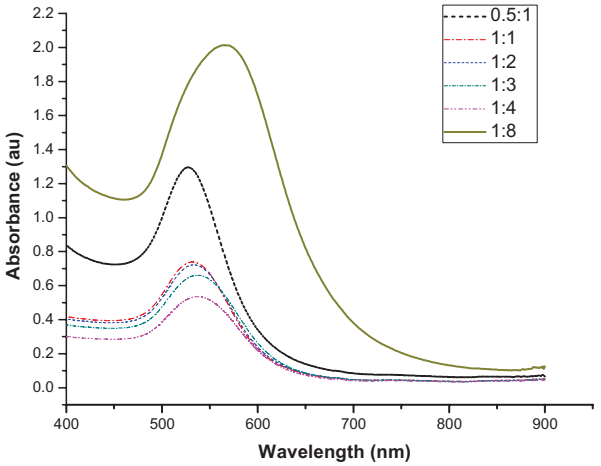

Figure 2 UV-Vis absorption spectra of GNPs with different ratios of $HAuCl_4$/BPEI (from 0.5:1 to 1:8).
Abbreviations: GNPs, gold nanoparticles; BPEI, branched polyethyleneimine.

of ~700 nm did not exist,[30] demonstrating that the majority of the GNPs were uniform sphere-like particles.[31] However, when the molar concentration of BPEI was increased to eight times that of $HAuCl_4$, the absorbance peak showed a significant red shift, far away from the characteristic absorption peak of GNPs. Thus, excess BPEI served as a linker bridging different particles into dimer or trimer aggregates.

In addition, the average diameter of GNPs increased as the BPEI concentration increased, as shown in Figure 3. When the mixture ratios of $HAuCl_4$ and BPEI were between 0.5:1 and 1:4, the size distributions of the GNPs were uniform. When the ratio reached 1:8, the average size of GNPs achieved micron levels with a dispersing and nonuniform distribution.

To conjugate more ALA onto cationic GNPs, we expected that GNPs would have more positive potential to attract ALA with negative charge. As illustrated in Figure 4, the zeta-potential increased with BPEI concentration within a certain range. However, when excessive BPEI (1:8) induced aggregates, the zeta-potential became negative. We chose to prepare ALA–GNP conjugates at a 1:4 ratio because these kinds of GNPs are similar in size to 1:3 conjugates, but are more positively charged and thus conjugate ALA more readily.

Characterization of ALA-GNP conjugates

ALA, a zwitterion, can have either an end group of COO^- or $NH3^+$, depending on the solution pH.[32] At physiological pH (7.2–7.6), its net negative charge enables conjugation to cationic GNPs through static electronic interactions.[14]

ALA was added to GNPs at various concentrations and the corresponding zeta-potentials were obtained at a solution pH of 7.4, as shown in Figure 5. As ALA concentration was increased, the zeta-potential of the GNPs decreased. This also confirmed that ALA had conjugated onto GNPs.

The stability of ALA-GNPs based on the sharp decrease in the zeta-potential indicates that the particles may be unstable.

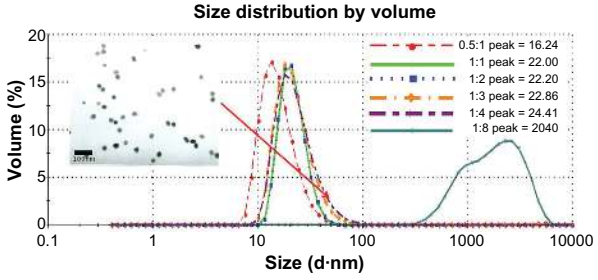

Figure 3 Size distribution of GNPs with different ratios of $HAuCl_4$/BPEI (from 0.5:1 to 1:8). Peak is the size of gold nanoparticles. Inset is the TEM micrograph of gold nanoparticles (1:4).
Abbreviations: BPEI, branched polyethyleneimine; GNPs, gold nanoparticles; TEM, transmission electron microscopy.

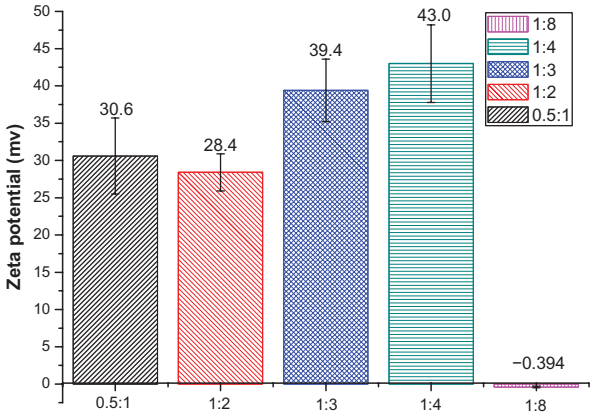

Figure 4 Zeta potential of GNPs with different ratios of $HAuCl_4$/BPEI (from 0.5:1 to 1:8).
Abbreviations: BPEI, branched polyethyleneimine; GNPs, gold nanoparticles.

However, the amine groups of BPEI, which associate with the particle surface, caused steric hindrance to prevent the aggregation of conjugates.[33] This was confirmed by measurements of the size distribution, as shown in Figure 6. Even when the concentration of the added ALA was increased to 8 mM, the average size of the conjugations did not change significantly. Thus, the addition of ALA did not induce the aggregation of conjugates.

Dark toxicity

The dark toxicity was investigated to determine whether the GNPs and ALA-GNP conjugates would affect the viability of K562 cells. The cell viability of dark treatment is shown in Figure 7, where cell viability is the optical density value of various drug treated groups in serum-free medium for 24 hours divided by that of the groups for 0 hours.

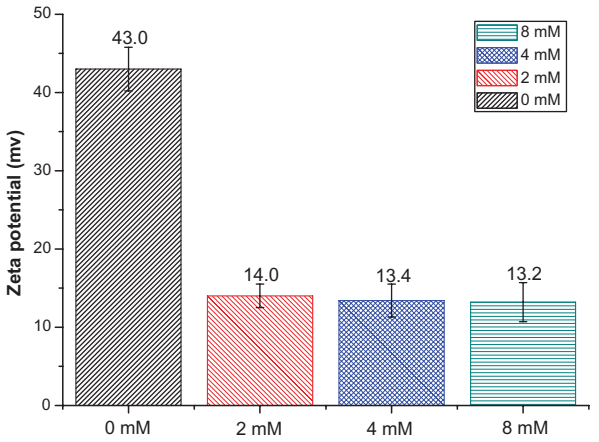

Figure 5 Zeta potential of ALA conjugated 1:4 ratio gold nanoparticles (1:4 GNPs) with different concentrations of ALA (from 0 mM to 8 mM).
Abbreviations: ALA, aminolevulinic acid; GNPs, gold nanoparticles.

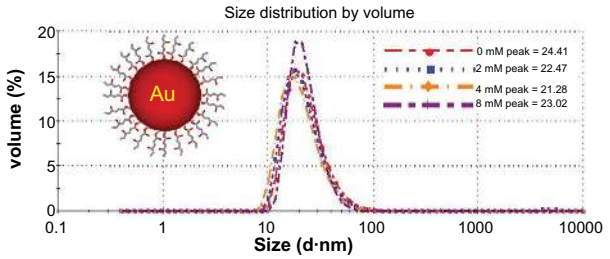

Figure 6 Size distribution of ALA (from 0 mM to 8 mM) conjugated gold nanoparticles (1:4 GNPs).
Notes: Peak is the size of gold nanoparticles. Inset is the scheme of ALA-conjugated gold nanoparticles.
Abbreviations: ALA, aminolevulinic acid; GNPs, gold nanoparticles.

There were no significant differences between the drug-treated groups and the untreated group.

PDT using ALA-GNP conjugates

As described earlier, PSs and light sources are both key elements that influence the efficacy of PDT. Therefore, we incubated K562 cell lines with ALA-GNP conjugates, ALA, or GNPs, and irradiated them with light sources to comprehensively analyze the effects of ALA-GNP conjugates and light conditions. In order to understand the interference of additional drugs, cell viability was characterized based on a normalized value, the OD value of the light-treatment group divided by that of the corresponding dark control group.

Cell viabilities after irradiation treatment are shown in Figure 8. ALA-GNP conjugates showed greater cytotoxicity against tumor cells than ALA alone under irradiation with various light sources. Moreover, GNPs alone had no significant effect on cell viability under irradiation. However, different light sources influenced the efficacy of PDT differently. For the control group without drug treatment, cell viability after purple LED irradiation decreased to 91.28%, which was lower than that after irradiation with a red or green LED. UV exposure itself may induce cell death and potentially harm normal cells. This conjecture is supported by the observation that the cell viability after exposure to filtered 410-nm light from the mercury lamp decreased to 85.89%. Therefore, the purple LED and mercury lamp was not the optimal light source due to its UV effects on normal cells.

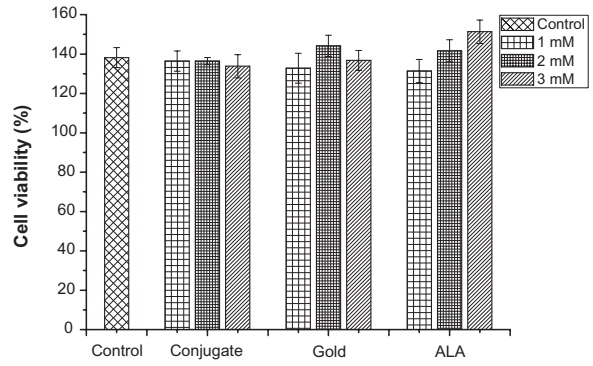

Figure 7 Viability of K562 cell under dark treatment.
Note: The data are representative of three duplicated experiments.

In addition to comparing the different effects of irradiation with various light sources for the control group, the effects of drug treatment on cell viability were also significantly different. As shown in Figure 8, although red and green LEDs did not significantly influence cell viability for the control group, cell viability with drug treatment was different after irradiation with these LED light sources. Comparing the control group with 2 mM 5-ALA-GNP treatment, cell viability decreased to 29.87% for 2 mM 5-ALA-GNPs under irradiation with green LEDs, but cell viability only decreased to 70.31% for 2 mM 5-ALA-GNPs under irradiation with red LEDs.

As shown in Figure 8C, although cell viability decreased to 51.62% for 1 mM 5-ALA-GNP treatment under irradiation with green LEDs in PDT, cell viability decreased with increasing concentrations of 5-ALA-GNPs and ALA. The group treated with 2 mM and 3 mM 5-ALA-GNP showed better inactivation than the group treated with the same concentration of ALA. Hence, green LEDs are the optimal light sources for enhancing the effects of 5-ALA-GNPs in PDT, with the group given 2 mM 5-ALA-GNPs showing the greatest inactivation under irradiation with green LEDs.

PpIX formation and detection

To determine the factors by which GNPs enhance the inactivating effects of ALA, we first investigated whether GNPs could affect PpIX formation. Medium containing 2 mM ALA, GNPs, or ALA-GNP conjugates was added to K562 cells with identical cell densities and incubated for different times. After thorough washing with PBS to remove free drug, the cells were lysed and centrifuged. Figure 9, which shows the fluorescence measurement of the intracellular PpIX formed from 5-ALA, indicated that the intracellular accumulation of PpIX in K562 was time-dependent. Maximum accumulation was observed at approximately 4–6 h after the addition of 5-ALA or 5-ALA-GNPs. Although the fluorescence intensity of the conjugate group was higher than that of the ALA group after 6 hours of incubation, this cannot explain why irradiation under red light has a lower inactive effect than other light sources. Therefore, enhancing the uptake of ALA with GNPs was not the only factor that resulted in a

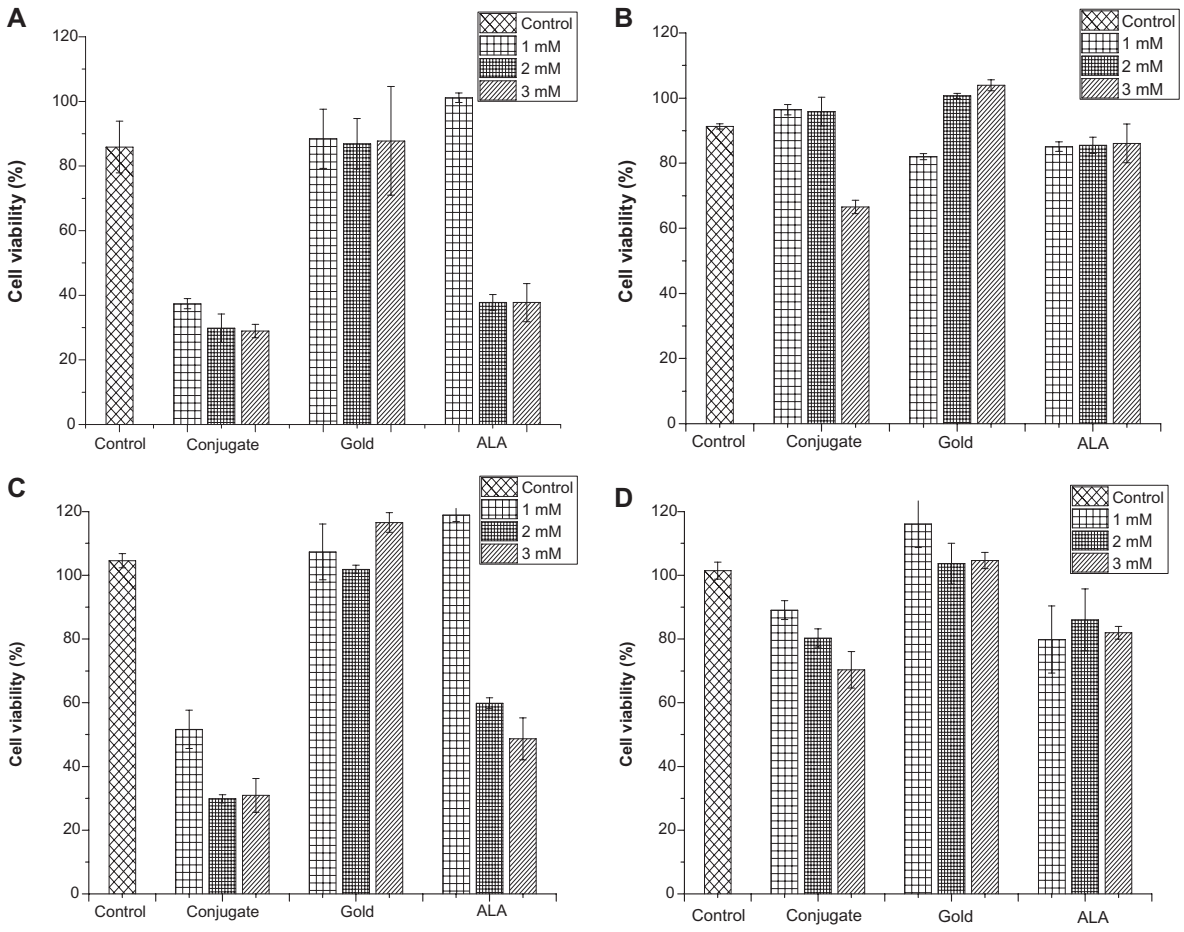

Figure 8 Viability of K562 cell after irradiation of various light sources. CCK-8 assay were performed when incubated 24 h after irradiation with (**A**) mercury arc lamp; (**B**) purple light LED; (**C**) green light; (**D**) red light LED.
Notes: Cell viability of their controls with no drug is also shown. The data are representative of three duplicated experiments.
Abbreviations: CCK-8, Cell Counting Kit 8; LED, light-emitting diode.

higher inactivation effect of 5-ALA-GNPs in the treatment of the cells.

Singlet oxygen measurement

We considered whether the photosensitization of PpIX was improved by GNPs due to PpIX producing more singlet oxygen. ALA is a precursor of the photosensitizer PpIX, which is the reaction agent in PDT. Therefore, we directly used PpIX to detect the influence of GNPs on singlet oxygen generation. Singlet oxygen is a short-lived species and can easily lose its energy by emitting light or internal conversion into heat.[34] Given the difficulty of directly measuring singlet oxygen generation, we used SOSGR, which emits green fluorescence at 525 nm in the presence of singlet oxygen, as the singlet oxygen sensor. The intensity of the green fluorescent signal could then be correlated with singlet oxygen concentration without signals from other reactive oxygen species.

Figure 10 shows the time-dependent fluorescence intensity of SOSGR with various treatments. GNPs clearly enhance the singlet oxygen generation of PpIX under exposure to green LEDs. The fluorescence response of SOSGR to GNPs is absent in controls with only GNPs or no drugs. However, singlet oxygen generation is limited under red LED exposure. These results provide a possible explanation for the better efficacy of ALA-GNP conjugates under irradiation with green LEDs in PDT.

Discussion

In this study, cationic GNPs were synthesized simply by heating an aqueous solution of $HAuCl_4$ and the polyelectrolyte BPEI without the addition of additional reductants. By controlling the molar ratio of $HAuCl_4$ and BPEI at 1:4, optimal GNPs with a zeta-potential of +43.0 mV were obtained to conjugate with ALA (Figure 4). Due to steric hindrance of BPEI, ALA was conjugated with GNPs

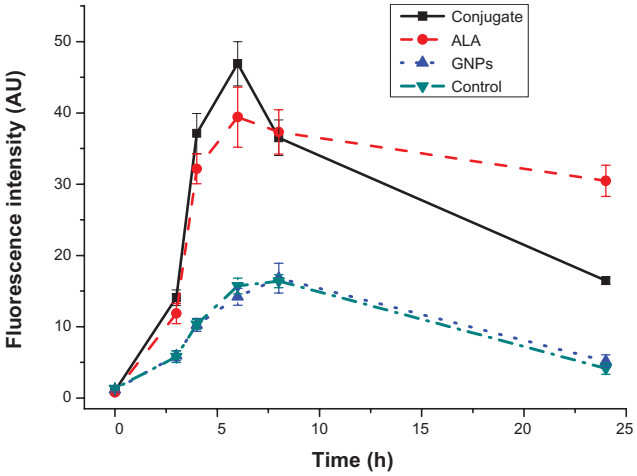

Figure 9 Intracellular formation of protoporphyrin IX is time-dependent.
Notes: The peak fluorescence value at 631 nm was used for kinetic measurement and an excitation of 410 nm on K562 cell incubated with GNPs, ALA and ALA-GNPs for various times.
Abbreviations: ALA, aminolevulinic acid; GNPs, gold nanoparticles.

without aggregation, even at 8 mM, while maintaining a positive potential (Figure 5).

Tumor cells have a lower negative zeta-potential in the cell membrane than do healthy cells, which should enhance the binding of positively charged ALA-GNPs to negatively charged K562 cells.[35] Additionally, ALA displays high selectivity for tumor cells due to enhanced selectivity of PpIX accumulation in malignant lesions.[36] Given this dual selectivity for tumor cells, ALA-GNPs should have better targeting effects than other photosensitive drugs.

In addition to identifying the optimum selectivity for tumor cells, the results of PDT indicated that GNPs can enhance the inactivation effects of ALA. One reason may be that GNPs act as water-soluble and biocompatible carriers that allow delivery of ALA through the cell membrane to synthesize PpIX, consistent with the observation that PpIX formation is detected. Hence, when the same concentration of ALA and ALA-GNPs were added to the cells, more ALA was synthesized into PpIX in the 5-ALA-GNP treatment group, and the accumulated PpIX induced significantly more photosensitization.[37]

However, this cannot explain why irradiation with different light sources produces different inactivation effects. For efficient photochemical reactions, matching the PS absorption with light emission spectra is crucial for obtaining higher photon absorption yields.[38] The absorption of the PS is an important parameter of the "total effective fluence."[39] Its absorption spectrum indicates that PpIX has the highest

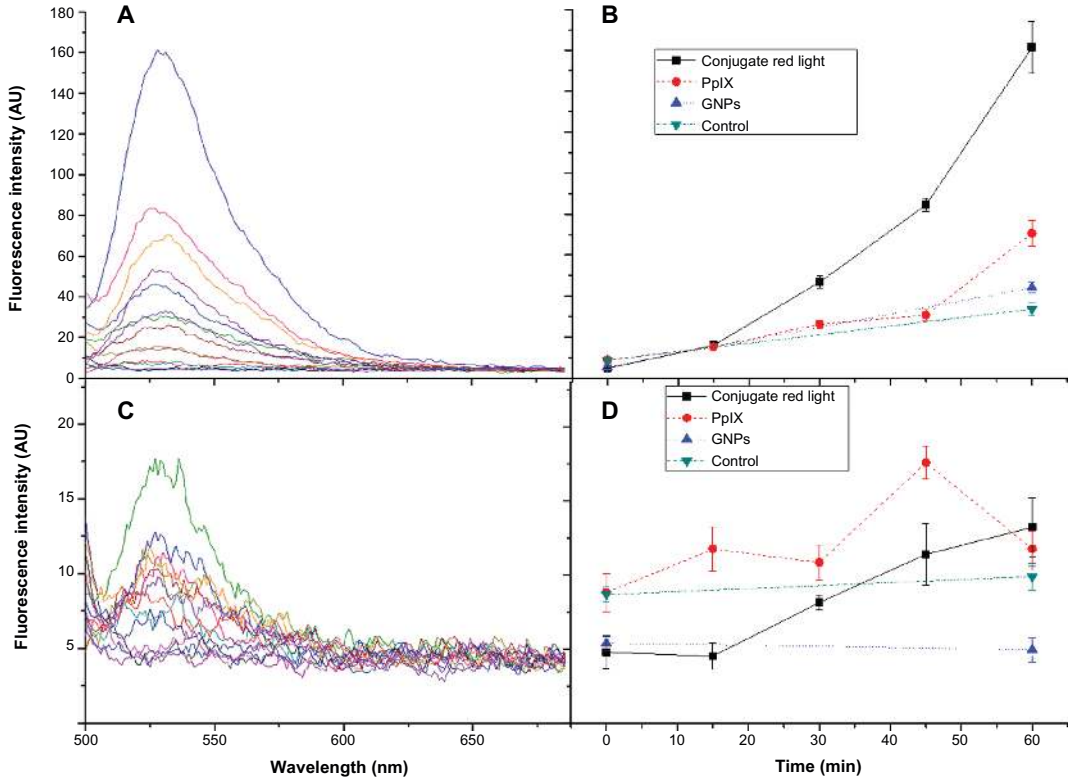

Figure 10 Fluorescence response of SOSGR to singlet oxygen as a function of time. The irradiation treatment was performed by illuminating the samples with (**A**) and (**B**) the fluorescence spectra of green light LED; (**C**) and (**D**) the fluorescence spectra of red light LED.
Abbreviations: GNPs, gold nanoparticles; LED, light-emitting diode; SOSGR, Singlet Oxygen Sensor Green reagent.

absorption peak at 404 nm, the second highest peak at 548 nm, and the lowest peak at 642 nm in phosphate buffer (pH 7).[40] Some studies have demonstrated that blue or green light is more potent than red light in activating PpIX.[39,41] The same PDT result in our study (Figure 8) also demonstrated that the mercury lamp (central wavelength = 395 nm) and two types of LEDs (central wavelength = 399 nm, 502 nm) were more effective than the red LED (central wavelength = 621 nm). The reason that most researchers have chosen a red light for PDT relates to the depth tissue, as an increased amount of red light is absorbed at greater depths. In addition, Mosely has calculated that green light gives the highest effective fluence before the tumor extends to 2.0 mm.[39]

Although the absorption of PpIX can explain why red light does not have high effective fluence, it cannot fully explain the ALA-GNP conjugates in our study. According to the absorption spectrum of PpIX, the absorption peak at 548 nm is lower than that at 404 nm. However, the mercury lamp (central wavelength = 395 nm) and LED (central wavelength = 502 nm) show similar levels of K562 cell destruction by ALA-GNP conjugates. According to the PDT mechanism,[42,43] an important factor responsible for the destruction of target cells is singlet oxygen.[2] Comparing the singlet oxygen measurements in our study, we postulate that the emission spectrum of green light fits with the absorption peak of GNPs (Figure 2) to induce an increase in the net system absorption of PpIX and enhance the photocurrent between GNPs and PpIX after light irradiation. Through nonradiative energy transfer and coupling to the surface plasmons of GNPs, more PSs are excited to their triplet and singlet states, which results in more singlet oxygen generation.[44] However, the emission spectra of other light sources do not fit with the absorption peak of GNPs. Hence, they cannot cause a strong surface plasmon effect to occur in GNPs.

Conclusion

This study aimed to combine PDT with nanotechnology by using a novel ALA-GNP conjugation technique to improve PDT efficacy. Through a comprehensive study on the preparation of ALA-GNP conjugates, light source adoption, and cell viability measurements, we conclude that ALA can be conjugated to GNPs and that the conjugation leads to a significant improvement in PDT efficacy. Using these conjugates as delivery vehicles, GNPs induced more ALA transport into the cell, thereby enhancing the effect of ALA-PDT because the hydrophilic nature of ALA limits its ability to penetrate cell membranes. In addition, GNPs noticeably enhanced singlet oxygen generation, which also led to a high efficacy of tumor cell destruction. This enhancement may result from the surface plasmon resonance that leads to increased net system absorption and triplet yield of PSs.

Based on parallel experiments with four light sources, we concluded that UV light has an inhibitory action on cell viability, possibly by causing normal cell death. Green light is optimal for conjugation-PDT; it has the best efficacy because green light itself does not harm cells.

ALA-GNP conjugation offers a new modality for efficient destruction of tumor cells. With the cooperation of a suitable light source with matching wavelength and sufficient power, ALA-GNP conjugation has great potential for enhancing cancer treatment with PDT. Nevertheless, significant advancement in related areas requires a full understanding of ALA-GNP accumulation in cell compartments. In addition, the role of plasmonic properties of GNPs in conjugation-PDT requires further investigation.

Acknowledgments/disclosure

The authors report no conflicts of interest in this work. The study was supported by the National Natural Science Foundation of China (61120106013, 60927011, 61108079, 60878056, 11274249).

References

1. Agostinis P, Berg K, Cengel KA, et al. Photodynamic therapy of cancer: an update. *CA Cancer J Clin*. 2011;61(4):250–281.
2. Dolmans DE, Fukumura D, Jain RK. Photodynamic therapy for cancer. *Nat Rev Cancer*. 2003;3(5):380–387.
3. Foster TH, Murant RS, Bryant RG, Knox RS, Gibson SL, Hilf R. Oxygen consumption and diffusion effects in photodynamic therapy. *Radiat Res*. 1991;126(3):296–303.
4. Brown SB, Brown EA, Walker I. The present and future role of photodynamic therapy in cancer treatment. *Lancet Oncol*. 2004;5(8):497–508.
5. Berkovitch G, Doron D, Nudelman A, Malik Z, Rephaeli A. Novel multifunctional acyloxyalkyl ester prodrugs of 5-aminolevulinic acid display improved anticancer activity independent and dependent on photoactivation. *J Med Chem*. 2008;51(23):7356–7369.
6. Kauppinen R. Porphyrias. *Lancet*. 2005;365(9455):241–252.
7. Kuelová K, Grebeová D, Pluskalová M, Marinov I, Hrkal Z. Early apoptotic features of K562 cell death induced by 5-aminolaevulinic acid-based photodynamic therapy. *J Photochem Photobiol B*. 2004;73(1–2):67–78.
8. Rodriguez L, Batlle A, Di Venosa G, et al. Study of the mechanisms of uptake of 5-aminolevulinic acid derivatives by PEPT1 and PEPT2 transporters as a tool to improve photodynamic therapy of tumours. *Int J Biochem Cell Biol*. 2006;38(9):1530–1539.
9. Daniel MC, Astruc D. Gold nanoparticles: assembly, supramolecular chemistry, quantum-size-related properties, and applications toward biology, catalysis, and nanotechnology. *Chem Rev*. 2004;104(1):293–346.
10. Shukla R, Bansal V, Chaudhary M, Basu A, Bhonde RR, Sastry M. Biocompatibility of gold nanoparticles and their endocytotic fate inside the cellular compartment: a microscopic overview. *Langmuir*. 2005;21(23):10644–10654.

11. Connor EE, Mwamuka J, Gole A, Murphy CJ, Wyatt MD. Gold nanoparticles are taken up by human cells but do not cause acute cytotoxicity. *Small*. 2005;1(3):325–327.
12. Ghosh P, Han G, De M, Kim CK, Rotello VM. Gold nanoparticles in delivery applications. *Adv Drug Deliv Rev*. 2008;60(11):1307–1315.
13. Hone DC, Walker PI, Evans-Gowing R, et al. Generation of cytotoxic singlet oxygen via phthalocyanine-stabilized gold nanoparticles: a potential delivery vehicle for photodynamic therapy. *Langmuir*. 2002; 18(8):2985–2987.
14. Oo MKK, Yang X, Du H, Wang H. 5-aminolevulinic acid-conjugated gold nanoparticles for photodynamic therapy of cancer. *Nanomedicine (Lond)*. 2008;3(6):777–786.
15. Cheng Y, Samia AC, Li J, Kenney ME, Resnick A, Burda C. Delivery and efficacy of a cancer drug as a function of the bond to the gold nanoparticle surface. *Langmuir*. 2010;26(4):2248–2255.
16. Wieder ME, Hone DC, Cook MJ, Handsley MM, Gavrilovic J, Russell DA. Intracellular photodynamic therapy with photosensitizer-nanoparticle conjugates: cancer therapy using a 'Trojan horse'. *Photochem Photobiol Sci*. 2006;5(8):727–734.
17. Jain KK. Nanotechnology-based drug delivery for cancer. *Technol Cancer Res Treat*. 2005;4(4):407–416.
18. Goodrich GP, Bao L, Gill-Sharp K, Sang KL, Wang J, Payne JD. Photothermal therapy in a murine colon cancer model using near-infrared absorbing gold nanorods. *J Biomed Opt*. 2012;15(1):018001.
19. Maeda H, Fang J, Inutsuka T, Kitamoto Y. Vascular permeability enhancement in solid tumor: various factors, mechanisms involved and its implications. *Int Immunopharmacol*. 2003;3(3):319–328.
20. Paciotti GF, Kingston DGI, Tamarkin L. Colloidal gold nanoparticles: a novel nanoparticle platform for developing multifunctional tumor–targeted drug delivery vectors. *Drug Dev Res*. 2006;67(1):47–54.
21. Yan F, Chen J, Ju H. Immobilization and electrochemical behavior of gold nanoparticles modified leukemia K562 cells and application in drug sensitivity test. *Electrochem Commun*. 2007;9(2):293–298.
22. Luo H, Li J, Chen X. Antitumor effect of N-succinyl-chitosan nanoparticles on K562 cells. *Biomed Pharmacother*. 2010;64(8):521–526.
23. Wang S, Gao R, Zhou F, Selke M. Nanomaterials and singlet oxygen photosensitizers: potential applications in photodynamic therapy. *J Mater Chem*. 2004;14:487–493.
24. Wang S, Yan J, Chen L. Formation of gold nanoparticles and self-assembly into dimer and trimer aggregates. *Mater Lett*. 2005;59(11): 1383–1386.
25. Schmidt MH, Meyer GA, Reichert KW, et al. Evaluation of photodynamic therapy near functional brain tissue in patients with recurrent brain tumors. *J Neurooncol*. 2004;67(1):201–207.
26. Zhang S, Zhang ZX. 5-aminolevulinic acid-based photodynamic therapy in leukemia cell HL60. *Photochem Photobiol*. 2004;79(6):545–550.
27. Kah JCY, Wan RCY, Wong KY, Mhaisalkar S, Sheppard CJR, Olivo M. Combinatorial treatment of photothermal therapy using gold nanoshells with conventional photodynamic therapy to improve treatment efficacy: an in vitro study. *Lasers Surg Med*. 2008;40(8):584–589.
28. Szeimies RM, Abels C, Fritsch C, et al. Wavelength dependency of photodynamic effects after sensitization with 5-aminolevulinic acid in vitro and in vivo. *J Invest Dermatol*. 1995;105(5):672–677.
29. Rao CNR, Kulkarni GU, Thomas PJ, Edwards PP. Metal nanoparticles and their assemblies. *Chem Soc Rev*. 2000;29(1):27–35.
30. Kuo WS, Chang CN, Chang YT, et al. Gold nanorods in photodynamic therapy, as hyperthermia agents, and in near-infrared optical imaging. *Angew Chem Int Ed Engl*. 2010;49(15):2771–2775.
31. Eustis S, El-Sayed M. Why gold nanoparticles are more precious than pretty gold: Noble metal surface plasmon resonance and its enhancement of the radiative and nonradiative properties of nanocrystals of different shapes. *Chem Soc Rev*. 2006;35(3):209–217.
32. Merclin N, Beronius P. Transport properties and association behaviour of the zwitterionic drug 5-aminolevulinic acid in water. a precision conductometric study. *Eur J Pharm Sci*. 2004;21(2–3):347–350.
33. Paul M. Metal nanoparticles: double layers, optical properties, and electrochemisty. In: Klabunde KJ, editor. *Nanoscale Materials in Chemistry*. New York, NY: Wiley Online Library; 2001:121–169.
34. Li BH, Lin H, Chen D, Wang M, Xie S. Detection system for singlet oxygen luminescence in photodynamic therapy. *Chinese Optics Letters*. 2010;8(1):86–88.
35. Seyfert S, Voigt A, Kabbeck-Kupijai D. Adhesion of leucocytes to microscope slides as influenced by electrostatic interaction. *Biomaterials*. 1995;16(3):201–207.
36. Wachowska M, Muchowicz A, Firczuk M, et al. Aminolevulinic acid (ALA) as a prodrug in photodynamic therapy of cancer. *Molecules*. 2011;16(5):4140–4164.
37. Kim CH, Chung CW, Choi KH, et al. Effect of 5-aminolevulinic acid-based photodynamic therapy via reactive oxygen species in human cholangiocarcinoma cells. *Int J Nanomedicine*. 2011;6:1357–1363.
38. Gerola AP, Semensato J, Pellosi DS, et al. Chemical determination of singlet oxygen from photosensitizers illuminated with LED: new calculation methodology considering the influence of photobleaching. *J Photochem Photobiol A Chem*. 2012;232(15):14–21.
39. Moseley H. Total effective fluence: a useful concept in photodynamic therapy. *Laser Med Sci*. 1996;11(2):139–143.
40. Lozovaya GI, Masinovsky Z, Sivash AA. Protoporphyrin ix as a possible ancient photosensitizer: Spectral and photochemical studies. *Origins of Life and Evolution of Biospheres*. 1990;20(3–4):321–330.
41. Piacquadio DJ, Chen DM, Farber HF, et al. Photodynamic therapy with aminolevulinic acid topical solution and visible blue light in the treatment of multiple actinic keratoses of the face and scalp: investigator-blinded, phase 3, multicenter trials. *Arch Dermatol*. 2004; 140(1):41–46.
42. Peng Q, Berg K, Moan J, Kongshaug M, Neslandl JM. 5-Aminolevulinic acid-based photodynamic therapy: principles and experimental research. *Photochem Photobiol*. 1997;65(2):235–251.
43. Ericson MB, Grapengiesser S, Gudmundson F, et al. A spectroscopic study of the photobleaching of protoporphyrin IX in solution. *Lasers Med Sci*. 2003;18(1):56–62.
44. Zhang Y, Aslan K, Previte MJR, Geddes CD. Plasmonic engineering of singlet oxygen generation. *Proc Natl Acad Sci U S A*. 2008;105(6): 1798–1802.